Compositional dependence of the performance of poly(p-phenylene vinylene)

Mihailetchi, VD; Koster, Lambert; Blom, PWM; Melzer, C; de Boer, B; van Duren, JKJ; Janssen, RAJ; Mihailetchi, Valentin D.; Janssen, René A.J.

Published in:
Advanced Functional Materials

DOI:
10.1002/adfm.200400345

Publication date:
2005

Compositional Dependence of the Performance of Poly(*p*-phenylene vinylene):Methanofullerene Bulk-Heterojunction Solar Cells**

By *Valentin D. Mihailetchi*, *L. Jan Anton Koster*, *Paul W. M. Blom*,* *Christian Melzer*, *Bert de Boer*, *Jeroen K. J. van Duren*, and *René A. J. Janssen*

The dependence of the performance of OC_1C_{10}-PPV:PCBM (poly(2-methoxy-5-(3′,7′-dimethyloctyloxy)-*p*-phenylene vinylene):methanofullerene [6,6]-phenyl C_{61}-butyric acid methyl ester)-based bulk heterojunction solar cells on their composition has been investigated. With regard to charge transport, we demonstrate that the electron mobility gradually increases on increasing the PCBM weight ratio, up to 80 wt.-%, and subsequently saturates to its bulk value. Surprisingly, the hole mobility in the PPV phase shows an identical behavior and saturates beyond 67 wt.-% PCBM, a value which is more than two orders of magnitude higher than that of the pure polymer. The experimental electron and hole mobilities were used to study the photocurrent generation of OC_1C_{10}-PPV:PCBM bulk-heterojunction (BHJ) solar cells. From numerical calculations, it is shown that for PCBM concentrations exceeding 80 wt.-% reduced light absorption is responsible for the loss of device performance. From 80 to 67 wt.-%, the decrease in power conversion efficiency is mainly due to a decreased separation efficiency of bound electron–hole (e–h) pairs. Below 67 wt.-%, the performance loss is governed by a combination of a reduced generation rate of e–h pairs and a strong decrease in hole transport.

1. Introduction

Organic solar cells based on a phase-separated mixture of donor and acceptor materials are a promising system for converting solar energy into electricity. Due to their light weight, low cost, ease of processing, and mechanical flexibility, these systems are an attractive alternative to inorganic solar cells. A successful approach is the bulk-heterojunction (BHJ)-type solar cell, prepared from blends of electron-donating conjugated polymer and electron-accepting fullerene molecules.[1] The functionality of devices of this type results from the ultrafast electron transfer from the conjugated polymer to the fullerene molecules.[2] To date, power conversion efficiencies of up to 2.5 % under air mass (AM) 1.5 illumination have been achieved for solar cells comprised of poly(2-methoxy-5-(3′,7′-dimethyloctyloxy)-*p*-phenylene vinylene), OC_1C_{10}-PPV, and methanofullerene [6,6]-phenyl C_{61}-butyric acid methyl ester (PCBM) as the electron donor and electron acceptor, respectively.[3] However, many fundamental questions concerning the operation of these devices and the processes limiting their performance still need to be addressed before a rational improvement of their performance can be established. In OC_1C_{10}-PPV:PCBM blends, light is mainly absorbed in the PPV phase; the PCBM plays the role of electron acceptor and electron-transport material. However, in order to obtain the maximum device efficiency, up to 80 wt.-% PCBM has to be added to the PPV:PCBM mixture. Since the PCBM percolation limit is expected to be only 17 vol.-%,[4,5] and conjugated polymers even show percolation at much lower fractions,[6] it is not clear why it should be necessary to add 80 wt.-% of a material that hardly contributes to the absorption of light (PCBM) in order to achieve optimal performance.

In a recent paper van Duren et al.[7] gave some useful insight on the interplay between film morphology and the performance of experimental solar cells. Using a variety of techniques they showed that, for OC_1C_{10}-PPV:PCBM, a rather homogeneous polymer matrix containing tiny PCBM crystals is present at up to 50 wt.-% PCBM. For concentrations higher than 67 wt.-% PCBM, the blend consists of large separate domains of pure PCBM embedded in a homogeneous matrix of 50:50 wt.-% PPV:PCBM. These large, almost pure PCBM domains grow on further increasing the PCBM concentration, thereby reducing the interface area between donor and acceptor where exciton dissociation takes place. In spite of this reduced interface area, the power conversion efficiency and fill factor were strongly enhanced when the PCBM ratio was increased from 67 to 80 wt.-%, and the phase-separated network developed. The origin of this enhancement has not yet been quantitatively explained.

Recently, we have developed a device model which consistently describes the behavior of PPV:PCBM BHJ solar cells with 80 wt.-% PCBM. The photocurrent in this cell is dominated by the dissociation efficiency of bound electron–hole (e–h) pairs at the donor–acceptor interface, which is a field-

[*] Prof. P. W. M. Blom, V. D. Mihailetchi, L. J. A. Koster, Dr. C. Melzer, Dr. B. de Boer
Materials Science Centre, University of Groningen
Nijenborgh 4, NL-9747 AG Groningen (The Netherlands)
E-mail: P.W.M.Blom@phys.rug.nl
Dr. J. K. J. van Duren, Prof. R. A. J. Janssen
Laboratory of Macromolecular and Organic Chemistry
Eindhoven University of Technology
PO Box 513, NL-5600 MB Eindhoven (The Netherlands)

[**] The authors thank J. C. Hummelen for supplying the PCBM and for fruitful discussions. These investigations were financially supported by the Dutch Ministries of EZ, O&W, and VROM through the EET program (EETK97115). The work of L. J. A. Koster forms part of the research program of the Dutch Polymer Institute (#323).

 DOI: 10.1002/adfm.200400345

and temperature-dependent process.[8] The device model calculates the steady-state charge distributions within the active layer by solving Poisson's equation and the continuity equations, including diffusion and recombination of charge carriers at the donor–acceptor interface.[9] Herein, we have applied the model to calculate the photocurrent of a series of devices of different OC_1C_{10}-PPV:PCBM compositions and quantify the parameters that limit device performance.

2. Results and Discussion

2.1. Compositional Dependence of the Charge-Carrier Mobility

After photoinduced electron transfer at the donor–acceptor interface, electrons are localized in the PCBM phase whereas the holes remain in the PPV polymer chains. Subsequently, the free electrons and holes must be transported via percolated PCBM and PPV pathways towards the electrodes to produce the photocurrent. Therefore, electron transport in PCBM and hole transport in PPV are crucial for understanding the opto-electronic properties of BHJ solar cells. For pure PCBM,[10] the electron mobility ($\mu_e = 2.0\times10^{-7}$ $m^2 V^{-1} s^{-1}$) is 4000 times higher than the hole mobility in pure OC_1C_{10}-PPV[11] ($\mu_h = 5.0\times10^{-11}$ $m^2 V^{-1} s^{-1}$). However, recently we found that the hole mobility in a 20:80 wt.-% OC_1C_{10}-PPV:PCBM blend is enhanced by more than two orders of magnitude compared to the pure polymer value.[12] As a result, the ratio between the electron and hole mobilities is reduced, typically to only a factor of ten, resulting in more balanced transport. Although the enhancement of the hole mobility by blending with PCBM is not yet fully understood, it clearly indicates that the hole and electron mobilities must be directly measured in the blend as used in the operational device. An extensive effort has been made to measure electron and hole transport in PPV:PCBM blends using time-of-flight photocurrent measurements,[13,14] and field-effect transistors,[15] and in both cases an enhancement of the hole mobility was observed. Recently, field-effect transistors have also been employed to measure the electron and hole mobilities in fullerene–oligophenyleneethynylene conjugates.[16] However, it should be noted that in field-effect transistors the hole mobility of OC_1C_{10}-PPV is three orders of magnitude larger than the hole mobility in light-emitting diodes or solar cells.[17] This enhancement is a result of the dependence of the mobility on charge-carrier density, which is orders of magnitude higher in a transistor than in a solar cell.[17] Therefore, realistic values for electron and hole mobilities can only be obtained when measuring them in the same device configuration as a light-emitting diode or solar cell.

The dark current in pure OC_1C_{10}-PPV and PCBM is space-charge limited (SCL),[10,11] allowing the direct determination of the mobility from current density–voltage (J–V) measurements. However, in blend devices, the presence of Ohmic contacts at both interfaces will result in a SCL current, which is a combination of both electron and hole current. Consequently, in order to measure the SCL current of only one type of charge carrier, the other one must be suppressed by a large injection barrier, resulting in an electron- or hole-only device. This approach has been successfully used to measure the hole-only SCL current in a 20:80 wt.-% OC_1C_{10}-PPV:PCBM blend when palladium was employed as the top electrode.[12] A schematic band diagram of such a hole-only device is depicted in Figure 1b. Employing palladium leads to an injection barrier of ≈0.95 eV for electrons in the PCBM conduction band, which sufficiently suppresses the injection of electrons into PCBM.[18]

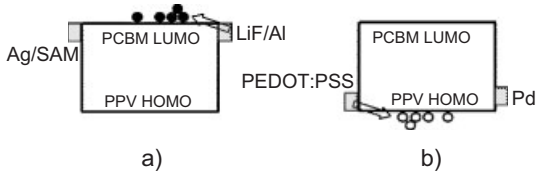

Figure 1. Schematic band diagram of the OC_1C_{10}-PPV:PCBM blends for a) the electron-only device and b) the hole-only device used in this study. Under forward bias, the arrows indicate the contact that injects electrons (a) or holes (b).

In order to suppress hole injection into OC_1C_{10}-PPV, the bottom contact must have a low work function. However, low-work-function metals (e.g., calcium) react easily with the spin-coated organic layer on top. To solve this issue, we modified the work function of the noble metal silver by using polar molecules that can self-assemble on the metal and form a highly ordered (two-dimensional) thin layer with a dipole in the desired direction.[19] Using a self-assembled monolayer (SAM) of hexadecanethiol on a flat 20 nm layer of silver lowered its work function by 0.6 eV to 3.8 eV,[20] as measured by a Kelvin probe. In Figure 1a, the schematic band diagram of such an electron-only device, using a modified bottom contact, is shown. From the work function of the Ag/SAM and highest occupied molecular orbital (HOMO) level of PPV, a hole-injection barrier of ≈1.3 eV is expected. This large injection barrier suppresses the hole current very efficiently, such that even in a blend with a low PCBM ratio and reduced electron transport the current is still electron dominated. In this way electron- and hole-only devices were constructed that enabled us to measure the SCL currents of electrons or holes separately in OC_1C_{10}-PPV:PCBM blends of various composition.

Figure 2 shows the experimental dark current densities (J_D) of OC_1C_{10}-PPV:PCBM blends that were measured in electron-only (Fig. 2a) and hole-only (Fig. 2b) devices for different wt.-% of PCBM. For clarity, only three compositions of both types of device are shown. On the horizontal axis, the applied voltage V was corrected for the built-in voltage (V_{BI})[21] and the voltage drop (V_{RS}) across the indium tin oxide/poly(3,4-ethylenedioxythiophene):poly(styrene sulfonic acid) (ITO/PEDOT:PSS) series resistance, which is typically 33 Ω in our substrates. At low voltages, J_D throughout all devices was found to scale quadratically with voltage, indicative of SCL transport. Similar to the findings for pure PCBM[10] and OC_1C_{10}-PPV,[11] at high voltages the mobility was taken to be dependent of the electric field (E) in stretched exponential form $\mu_{e,h}(E) = \mu_{e,h}(0)\exp(\gamma_{e,h}E^{1/2})$, where $\mu_{e,h}(0)$ is the zero-field mobility of electrons

ADVANCED FUNCTIONAL MATERIALS

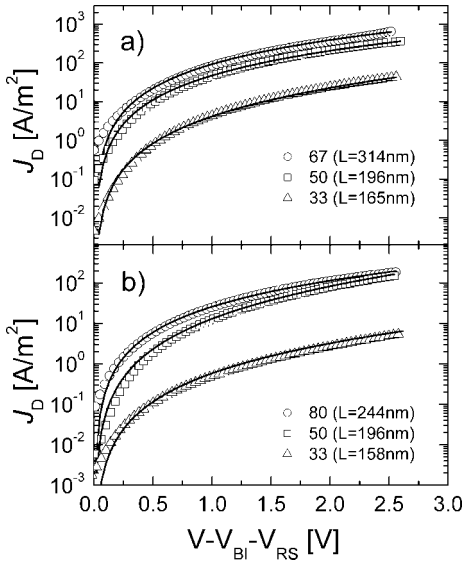

Figure 2. Experimental dark-current densities for OC_1C_{10}-PPV:PCBM devices (see legend) with varying wt.-% PCBM, for a) an electron-only device, and b) a hole-only device. The solid lines represent the fit using a model of single carrier SCL current with field-dependent mobility. The J_D–V characteristics are corrected for the voltage drop over the contacts V_{RS} and for the built-in voltage V_{BI} that arises from the work function difference between the contacts. The film thicknesses L for each composition are also shown.

and holes, respectively, and $\gamma_{e,h}$ is the field-activation factor. The experimental data in Figure 2 were fitted using the model of a single carrier SCL current[10] with field-dependent mobility, and the results are shown by the solid lines.

The calculated zero-field mobility of electrons and holes in OC_1C_{10}-PPV:PCBM BHJ devices are presented as a function of wt.-% PCBM in Figure 3. A gradual increase of electron mobility with increasing fullerene concentration was observed from 33 to 80 wt.-%, followed by saturation to the value of pure PCBM (2×10^{-7} m^2 V^{-1} s^{-1}).[10] This saturation does not coincide with the start of the phase separation ($\approx$67 wt.-%),[7] but rather occurs at the maximum device performance. Surprisingly, the hole mobility shows a similar behavior as a function of fullerene concentration. Intuitively, one would expect that

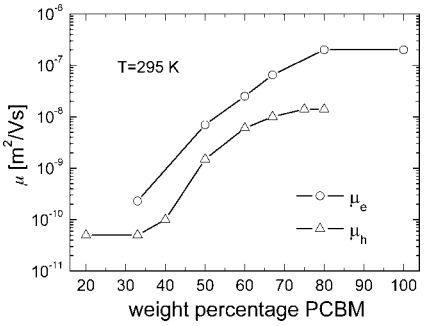

Figure 3. Electron and hole zero-field mobilities in blends of OC_1C_{10}-PPV:PCBM as a function of PCBM weight percentage, at room temperature (295 K). The mobilities were calculated from the SCL current presented in Figure 2. The electron mobility for 100 wt.-% PCBM was taken from [10].

'dilution' of the PPV with PCBM would lead to a reduction of the hole-transport properties, for example due to a reduced percolation pathway. However, from 40 to 80 wt.-% PCBM the hole mobility increased by more than two orders of magnitude from its pure polymer value (5×10^{-11} m^2 V^{-1} s^{-1}) to approximately 1.4×10^{-8} m^2 V^{-1} s^{-1} in the blend. The origin of this strong increase is not yet clear. It has been shown that films of OC_1C_{10}-PPV exhibit interconnected ring-like features, due to asymmetric side chains.[22] This seems to be consistent with the proposition made by Pacios et al.[23] who proposed that the change in film morphology upon adding PCBM molecules results in an enhanced intermolecular interaction and, therefore, in an improved charge transfer between adjacent polymer chains. Based on this consideration, an enhancement in hole transport may be possible. For fullerene concentrations above 67 wt.-%, the hole mobility saturates. It has been pointed out by van Duren et al. that phase separation, resulting in pure PCBM domains surrounded by a homogeneous matrix of 50:50 wt.-% OC_1C_{10}-PPV:PCBM, sets in for concentrations above 67 wt.-% PCBM.[7] As a result, the hole mobility in this homogeneous matrix of 50:50 PPV:PCBM is indeed expected to saturate, as is observed experimentally in Figure 3. Thus, a clear connection between film morphology and charge transport has been established. In the next section, the experimental charge-carrier mobilities in OC_1C_{10}-PPV:PCBM blends are applied to analyze the photocurrent generation and performance of solar cells based on these blends.

2.2. Device Characterization under Illumination

Photocurrent generation in the PPV:PCBM BHJ devices is governed by a number of sequential processes: the generation of excitons after absorption of light by PPV, followed by exciton diffusion towards the polymer–fullerene (donor–acceptor) interface, and dissociation via ultrafast electron transfer. After dissociation, a geminate pair of a hole at the donor and an electron at the acceptor is formed. Due to the low dielectric constants ε_r of the organic materials (ε_r typically ranges from 2–4), these e–h pairs are strongly bound by Coulomb interactions, with typical binding energies of several tenths of an electron volt. In order to generate a photocurrent, the bound e–h pairs must dissociate into free charge carriers and subsequently move to the electrodes before recombination processes can take place.

Figure 4 shows the experimental photocurrent J_{ph} as a function of effective applied voltage (V_0–V) for three different OC_1C_{10}-PPV:PCBM compositions. The photocurrent (J_{ph}; $J_{ph}=J_L-J_D$) is the measured current under illumination (J_L) corrected for the dark current (J_D), whereas the compensation voltage V_0 is defined as the voltage at which the photocurrent J_{ph} is zero. Previously, we demonstrated that for 20:80 wt.-% OC_1C_{10}-PPV:PCBM composition at a voltage close to the compensation voltage V_0 ($V_0-V<0.1$ V), the photocurrent increases linearly with voltage. For $V_0-V>0.1$ V, the photocurrent enters a regime where it is dominated by the dissociation efficiency of the bound e–h pairs, which is a field- and tempera-

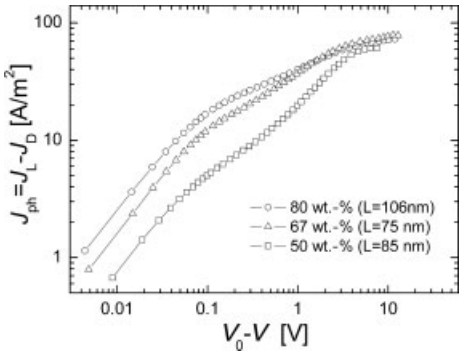

Figure 4. Experimental photocurrent as a function of effective applied voltage (V_0–V) for three different OC_1C_{10}-PPV:PCBM compositions (see legend). V_0 represents the compensation voltage for which the photocurrent $J_{ph}=J_L-J_D=0$.

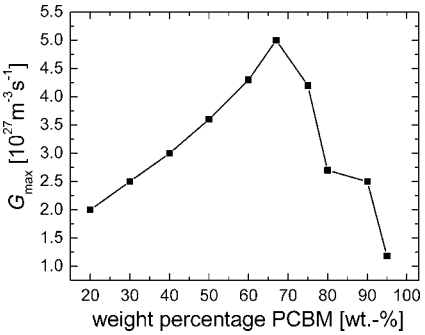

Figure 5. Calculated maximum generation rate of electron–hole pairs at the internal donor–acceptor interface in OC_1C_{10}-PPV:PCBM blends, as a function of wt.-% PCBM. G_{max} was calculated from the saturation of the photocurrent, as illustrated in Figure 4.

ture-dependent process.[8] The photocurrent of the 20:80 blend could consistently be described using a model based on Onsager's theory of ion pair dissociation, in which the dissociation probability $P(E,T)$ for a given electric field E and temperature T is calculated. It should be noted that the calculation of $P(E,T)$ requires, as input parameters, the lifetime of bound e–h pairs (k_F^{-1}), the spatial distribution of e–h pairs at the donor–acceptor interface, the dielectric constant, and the recombination rate constant (k_R) of free charge carriers. The latter has been considered to be of Langevin type[8] and describes the conversion of free carriers into bound pairs at the interface. Furthermore, as shown in Figure 4, the photocurrent in OC_1C_{10}-PPV:PCBM blends begins to saturate for all three compositions (J_{sat}) when subjected to a large reverse bias (≤ –10 V) and becomes field- and temperature-independent,[8] meaning that every e–h pair is dissociated into free charge carriers ($P\rightarrow1$). Since at full saturation $J_{sat}=qG_{max}L$, where q is the electric charge and L the film thickness, the occurrence of the saturated photocurrent allows us to calculate directly the maximum possible generation rate G_{max} for producing free carriers out of bound e–h pairs at the donor–acceptor interface for any PPV:PCBM composition. From J_{sat} (Fig. 4), one can directly observe that for 67 wt.-% PCBM more bound e–h pairs are produced in the active layer than for 50 or 80 wt.-%.

In Figure 5, G_{max} is shown as a function of weight percentage of PCBM for all compositions measured. Surprisingly, the maximum generation of e–h pairs at 67 wt.-% PCBM does not coincide with the maximum solar cell performance at 80 wt.-% PCBM. Furthermore, it is already known that a few weight percentage of PCBM is sufficient to quench nearly all photoluminescence in PPV. Thus, at low PCBM weight fractions, all excitons created in the PPV are already able to dissociate at a PPV:PCBM interface. Following this reasoning, one would expect that the number of photogenerated e–h pairs would simply decrease with increasing PCBM weight fraction due to a reduced absorption in the PPV. However, it should be noted that G_{max} represents the maximum number of bound e–h pairs that can contribute to the photocurrent. For low PCBM weight fractions, many free electrons cannot leave the device because they are located on isolated PCBM clusters, and will eventually recombine through the formation of a long-lived, bound e–h pairs at the interface. With increasing PCBM weight fraction, the number of percolation paths will increase, thereby increasing the number of electrons that can contribute to the photocurrent after being dissociated from the hole at the interface. At PCBM fractions larger than 67 wt.-%, the reduced absorption in the PPV will lead to a decrease in G_{max}.

An important question remains: why do these types of devices have their optimum performance at 80 wt.-% PCBM, despite the decrease in the number of photogenerated bound e–h pairs? In the saturation regime V_0–$V>0.1$ V, the photocurrent is basically given by $J_{ph}=eG_{max}P(E,T)L$, in which the dissociation efficiency $P(E,T)$ represents the field- and temperature-dependence of the generation rate.[8] In order to compare $P(E,T)$ with experimental data, the measured photocurrents from Figure 4 were normalized to their saturation value ($qG_{max}L$), as shown in Figure 6 for the 50 and 80 wt.-% PCBM devices. This normalized photocurrent then reflects the disso-

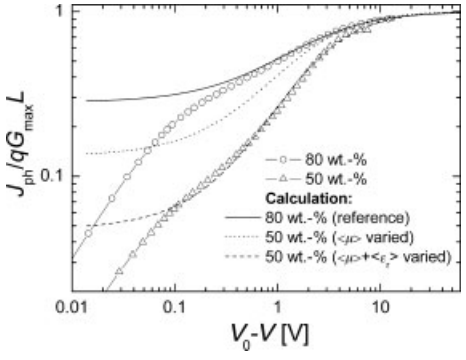

Figure 6. Experimental photocurrent normalized to its saturation value ($qG_{max}L$) as a function of effective applied voltage (V_0–V) for two different OC_1C_{10}-PPV:PCBM compositions (see legend). The lines represent the calculated dissociation probability of bound e–h pairs (P) at the donor–acceptor interface as follows: The solid line represents the calculated P that best fits the experimental data, with 80 wt.-% PCBM used as the reference. The dotted line denotes the calculated P for 50 wt.-% PCBM when only the charge-carrier mobilities $\langle\mu\rangle$ have been modified; the dashed line represents the same calculation for the case when both $\langle\mu\rangle$ and the bulk dielectric constant $\langle\varepsilon_r\rangle$ are modified.

ADVANCED FUNCTIONAL MATERIALS

ciation efficiency in the saturation regime for effective voltages V_0–$V > 0.1$ V. It appears that a decrease of the PCBM weight fraction from 80 to 50 wt.-% leads to a strong reduction of the dissociation efficiency in the relevant voltage regime (V_0–$V < 0.9$ V). The origin of this decrease in the dissociation efficiency of bound e–h pairs with decreasing PCBM concentration will now be further addressed. For low-mobility semiconductors, recombination of free charge carriers is given by Langevin as

$$k_R = q\langle\mu\rangle/\varepsilon_0\langle\varepsilon_r\rangle \quad (1)$$

where $\langle\varepsilon_r\rangle$ are the spatially averaged dielectric constants, 2.11 and 3.9 for OC_1C_{10}-PPV and PCBM, respectively (depending on their volume ratio), and $\langle\mu\rangle$ is the effective charge-carrier mobility of electrons and holes. The parameters in the model that vary with the PCBM fraction are k_F, ε_r, and k_R. Since the average dielectric constant and the charge-carrier mobilities are known at each composition (Fig. 3), k_F remains the only adjustable parameter in our calculation on changing the composition. The dissociation efficiency of the device with 80 wt.-% PCBM (Fig. 6, solid line) has been calculated before, and will be used as a reference.[8] From this calculation, a lifetime (k_F^{-1})of typically 2.5 μs was obtained, in agreement with absorption spectroscopy measurements where bound e–h pairs in PPV:PCBM blends can still be detected after microseconds and even milliseconds, depending on the temperature.[24–27] However, these photophysical studies and quantitative modeling suggest a multiphasic recombination dynamics of bound e–h pairs across the interface, which ranges from tens of nanoseconds to milliseconds.[24–27] It is difficult to reconcile these results with the calculated k_F^{-1} (≈2.5 μs) from our model. We note that the experimental conditions in transient absorption measurements differ strongly from the device studies. The photophysical experiments were performed at higher light intensity, charge density, and—most importantly—in the absence of an electric field. Whether these differences in experimental conditions explain the apparent discrepancy is the subject of further investigation.

Next, we systematically calculated *P(E,T)* for a device with 50 wt.-% PCBM, changing the input parameters of the 80 wt.-% device one-by-one. First, we adapted the charge-carrier mobilities and kept all other parameters constant. Figure 6 (dotted line) shows that the decrease in the electron and hole mobilities, despite being a drop of typically an order of magnitude for an 80 to 50 wt.-% decrease in PCBM (Fig. 3), is not solely responsible for the observed decrease in dissociation efficiency. Subsequently, besides the mobility, the change in the spatially averaged dielectric constant $\langle\varepsilon_r\rangle$, in accordance with the change in PPV and PCBM volume ratio, was also taken into account (dashed line). The calculated *P(E,T)* exactly fitted the experimental data (Fig. 6), without having to change any of the other parameters. Thus, the lower separation efficiency at 50 wt.-% PCBM results from the combination of a decreased charge-carrier mobility and lower dielectric constant, resulting in a stronger e–h binding energy. This result was then used to numerically model the experimental photocurrent of a series of OC_1C_{10}-PPV:PCBM blend devices with varying the PCBM compositions—from 20 to 95 wt.-%. Further detail on the numerical model, which includes *P(E,T)*, can be found in the literature.[9] The only input parameters that change with PCBM weight fraction are the mobilities (Fig. 3), G_{max} (Fig. 5), as obtained from the fully saturated part of the photocurrent, and the spatially averaged $\langle\varepsilon_r\rangle$. The other parameters used were identical to the fit of the 20:80 wt.-% device.[8] Figure 7 shows the J_L–V characteristics under illumination of a number of composite devices with varying weight percentage of PCBM in

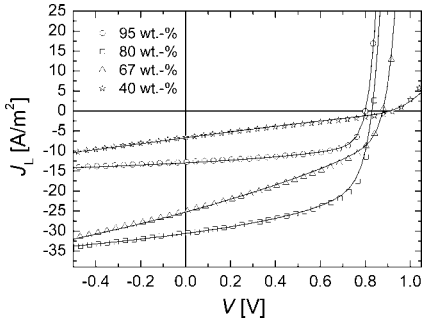

Figure 7. J_L–V characteristics under illumination of the ITO/PEDOT:PSS/OC_1C_{10}-PPV:PCBM/LiF/Al devices with varying wt.-% PCBM in OC_1C_{10}-PPV. The devices were illuminated using a tungsten–halogen lamp with a power intensity of 180 mW cm^{-2}. The solid lines represent the numerical calculation using a model [9].

OC_1C_{10}-PPV: the solid lines represent the numerical fits. The excellent agreement between simulations and experiments for all compositions demonstrate that the mobilities, maximum generation rate, and spatially averaged dielectric constant are the key parameters that govern the composition dependence of the performance of OC_1C_{10}-PPV:PCBM-based solar cells. It should be noted that, in the composition range 50 to 95 wt.-%, all calculations were done with a constant lifetime k_F^{-1} of 2.5 μs, whereas, for 40 wt.-%, a lifetime of 40 μs had to be used to fit the experimental data. At even lower fractions, the lifetime further increased. The exact origin of this increase in lifetime for low PCBM fractions is not yet clear, but its onset corresponds to the measured drop in hole transport. Whether the low mobility, which might hinder the holes from reaching the donor–acceptor interface, is responsible for this lifetime increase is the subject of further study.

From the excellent agreement between simulated and experimental photocurrent (Fig. 7), it directly follows that the model also accurately describes the experimental power conversion efficiency η (normalized to its maximum value η_{max}) and the fill factor (*FF*) as a function of wt.-% PCBM, as shown in Figure 8. Since the open-circuit voltage (V_{oc}) of these blends is merely related to the electronic levels of the donor and acceptor and the type of contacts used,[17] the variation in η is mainly due to a change in the short-circuit current (J_{sc}) and/or *FF*. For PCBM concentrations exceeding 80 wt.-%, the decrease in optical density of the film due to the poorer absorption of the PCBM compared to the OC_1C_{10}-PPV, combined with a reduced interface area between donor and acceptor,

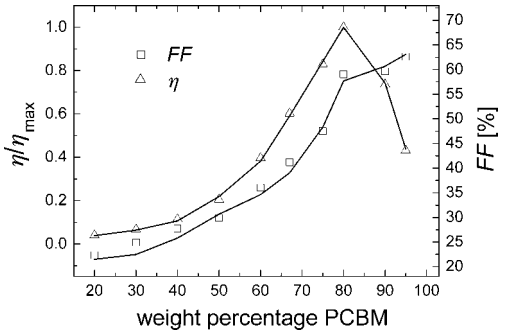

Figure 8. Experimental power conversion efficiency normalized to the maximum value and fill factor (see legend) with varying PCBM composition, at room temperature. The solid lines represent the numerical calculations.

results in a drop in the maximum generation rate G_{max} of e–h pairs. This will give rise to a decrease in J_{sc} and consequently η, despite the efficient charge separation and high *FF*. For example, the decrease by a factor of 2.3 in η (Fig. 8) between 80 and 95 wt.-% is entirely due to the decrease in G_{max} (Fig. 5).

The most interesting range for the device performance is from 80 to 67 wt.-%, where phase separation starts to develop. In this range, a drop in device efficiency by 40 % was measured, despite an increased G_{max}. Recently, we demonstrated that at short-circuit (SC) conditions in 20:80 wt.-% OC_1C_{10}-PPV:PCBM blends, only 60 % of the total e–h pairs that are generated at the donor–acceptor interface, after photoinduced electron transfer, are separated into free charge carriers and subsequently collected at the electrodes,[8] which is one of the important loss mechanisms in this material system. Figure 9 shows the calculated separation efficiency of e–h pairs at SC (η_{sc}) for all fitted OC_1C_{10}-PPV:PCBM compositions. η_{sc} strongly decreases for fullerene concentrations below 80 wt.-%, re-

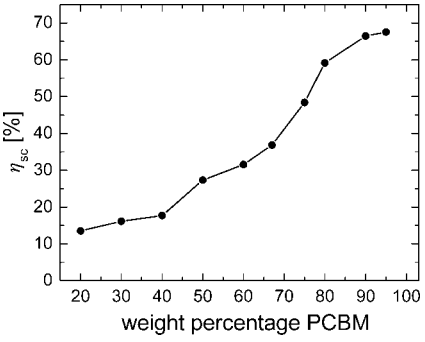

Figure 9. Calculated charge separation efficiency at short-circuit conditions as a function of weight percentage of PCBM.

sulting from the lower charge-carrier mobilities and lower dielectric constant (see Fig. 6). As a result, the benefit of a higher G_{max} at 67 wt.-% is completely compensated by a poorer η_{sc}: it is only 36.8 % at 67 wt.-% PCBM (Fig. 9). Below 67 wt.-%, G_{max} gradually decreases and, strengthened by a strong decrease in hole transport, the separation efficiency of bound e–h pairs is further reduced, which is detrimental for the device performance. As a consequence, the loss in the device performance below 67 wt.-% is due to a combined effect of a reduced G_{max}, weaker separation efficiency of bound e–h pairs from the donor–acceptor interface, and a strong decrease in the hole transport.

Consequently, the most important factor for obtaining the power efficiencies of 2.5 % presently reported for the OC_1C_{10}-PPV:PCBM blends is the enhancement of μ_h in the blend by more than two orders of magnitude, as compared to the pure OC_1C_{10}-PPV. Without such an enhancement, these efficiencies would not be possible in this material system, and the performance would be strongly limited by space-charge effects. The optimum performance at 80 wt.-% PCBM is governed by the best compromise between absorption (G_{max}), dielectric constant, $\langle\varepsilon_r\rangle$, and charge transport ($\mu_h$).

3. Conclusion

We have independently measured the electron and hole mobilities in OC_1C_{10}-PPV:PCBM blend films with varying PCBM concentrations. The electron mobility in the PCBM phase gradually increases with increasing fullerene concentration, up to 80 wt.-%, due to the increasing number of continuous percolated pathways from the bottom to the top electrode. Surprisingly, the hole mobility in OC_1C_{10}-PPV shows similar behavior as a function of fullerene concentration: from 40 wt.-%, it starts to increase from that of the pure OC_1C_{10}-PPV hole mobility and saturates beyond 67 wt.-%, at a value which is more than two orders of magnitude higher. This enhancement and its saturation are strongly related to recent findings on the morphology of these devices.

The resulting electron and hole mobilities were used to study the photocurrent generation of OC_1C_{10}-PPV:PCBM BHJ solar cells. Using a full numerical model to fit the experimental data, it was shown that, for PCBM concentrations of more than 80 wt.-%, the reduced light absorption and interface area between donor and acceptor is responsible for the poor device performance. From 80 to 67 wt.-%, the decrease in power conversion efficiency, despite an increase in the maximum generation rate of e–h pairs at the donor–acceptor interface, is due to the decrease in separation efficiency of bound e–h pairs from the donor–acceptor interface. Finally, below 67 wt.-%, the reduced generation rate and strong decrease in the hole transport further diminish the performance of this kind of solar cell.

4. Experimental

All solar cell devices used to investigate the photocurrent in this study were prepared using ITO-coated glass substrates. To supplement this bottom electrode, a hole-transport layer of PEDOT:PSS (Bayer AG) was spin-coated from an aqueous dispersion solution, under ambient conditions, before drying the substrates at 140 °C. Next, composite layers of OC_1C_{10}-PPV and PCBM were spin-coated from chlorobenzene solution on top of the PEDOT:PSS layer, with film thicknesses ranging from 75 to 130 nm. To complete the solar cell devices, 1 nm lithium fluoride topped with aluminum (110 nm) electrodes was deposited by thermal evaporation under vacuum (1×10^{-7} mbar;

ADVANCED FUNCTIONAL MATERIALS

1 mbar = 100 Pa). The current density versus voltage curves were measured in a N_2 atmosphere (< 1 ppm O_2 and < 1 ppm H_2O) at room temperature with a computer-controlled Keithley 2400 Source Meter. To measure the photocurrent (J_L), the devices were illuminated at the transparent ITO electrode by a white light tungsten–halogen lamp with an intensity of 180 mW cm^{-2}. The lamp light output was filtered by a Schott KG1 and GG385 filter resulting in a spectral range of 400–900 nm with its maximum at 650 nm. Light power was measured with an Ophir Laser Power Meter set at 610 nm. Energetically, the devices are approximated by the metal–insulator–metal picture [1], with the lowest unoccupied molecular orbital (LUMO) of the acceptor (PCBM) and the HOMO of the donor (OC_1C_{10}-PPV) as the conduction and valence bands, respectively.

Received: July 30, 2004
Final version: October 26, 2004

[1] C. J. Brabec, N. S. Sariciftci, J. C. Hummelen, *Adv. Funct. Mater.* **2001**, *11*, 15.
[2] N. S. Sariciftci, L. Smilowitz, A. J. Heeger, F. Wudl, *Science* **1992**, *258*, 1474.
[3] S. E. Shaheen, C. J. Brabec, N. S. Sariciftci, F. Padinger, T. Fromherz, J. C. Hummelen, *Appl. Phys. Lett.* **2001**, *78*, 841.
[4] A. Aharony, D. Stauffer, *Introduction to Percolation Theory*, 2nd ed., Taylor and Francis, London **1993**.
[5] S. Hotta, S. D. D. V. Rughooputh, A. J. Heeger, *Synth. Met.* **1987**, *22*, 79.
[6] A. J. Heeger, *Trends Polym. Sci.* **1995**, *3*, 39.
[7] J. K. J. van Duren, X. Yang, J. Loos, C. W. T. Bulle-Lieuwma, A. B. Sieval, J. C. Hummelen, R. A. J. Janssen, *Adv. Funct. Mater.* **2004**, *14*, 425.
[8] V. D. Mihailetchi, L. J. A. Koster, J. C. Hummelen, P. W. M. Blom, *Phys. Rev. Lett.* **2004**, *93*, 216 601.
[9] L. J. A. Koster, E. C. P. Smits, V. D. Mihailetchi, P. W. M. Blom, unpublished.
[10] V. D. Mihailetchi, J. K. J. van Duren, P. W. M. Blom, J. C. Hummelen, R. A. J. Janssen, J. M. Kroon, M. T. Rispens, W. J. H. Verhees, M. M. Wienk, *Adv. Funct. Mater.* **2003**, *13*, 43.
[11] P. W. M. Blom, M. J. M. de Jong, M. G. van Munster, *Phys. Rev. B: Condens. Matter* **1997**, *55*, R656.
[12] C. Melzer, E. Koop, V. D. Mihailetchi, P. W. M. Blom, *Adv. Funct. Mater.* **2004**, *14*, 865.
[13] S. A. Choulis, J. Nelson, Y. Kim, D. Poplavskyy, T. Kreouzis, J. R. Durrant, D. D. C. Bradley, *Appl. Phys. Lett.* **2003**, *83*, 3812.
[14] R. Pacios, J. Nelson, D. D. C. Bradley, C. J. Brabec, *Appl. Phys. Lett.* **2003**, *83*, 4764.
[15] W. Geens, S. E. Shaheen, C. J. Brabec, J. Poortmans, N. S. Sariciftci, in *Electronic Properties of Novel Materials—Molecular Nanostructures Euroconf.* (Eds: H. Kuzmany, J. Fink, M. Mehring, S. Roth), American Institute of Physics, Melville, NY **2000**, p. 516.
[16] J. F. Nierengarten, T. Gu, T. Aernouts, W. Geens, J. Poortmans, G. Hadziioannou, D. Tsamouras, *Appl. Phys. A.* **2004**, *79*, 47.
[17] C. Tanase, E. J. Meijer, P. W. M. Blom, D. M. de Leeuw, *Phys. Rev. Lett.* **2003**, *91*, 216 601.
[18] V. D. Mihailetchi, P. W. M. Blom, J. C. Hummelen, M. T. Rispens, *J. Appl. Phys.* **2003**, *94*, 6849.
[19] I. H. Campbell, S. Rubin, T. A. Zawodzinski, J. D. Kress, R. L. Martin, D. L. Smith, N. N. Barashkov, J. P. Ferraris, *Phys. Rev. B* **1996**, *54*, 14 321.
[20] B. de Boer, A. Hadipour, M. M. Mandoc, T. Van Woudenbergh, P. W. M. Blom, *Adv. Mater.*, in press.
[21] For hole-only devices, V_{BI} was taken as a compensation voltage $V_0 \approx V_{oc} + 0.05$ V, whereas for electron-only devices V_{BI} was estimated from the work function difference between Ag/SAM and LiF/Al contacts $V_{BI} \approx 0.2$ V.
[22] M. Kemerink, J. K. J. van Duren, P. Jonkheijm, W. F. Pasveer, P. M. Koenraad, R. A. J. Janssen, H. W. M. Salemink, J. H. Wolter, *Nano Lett.* **2003**, *3*, 1191.
[23] R. Pacios, D. D. C. Bradley, J. Nelson, C. J. Brabec, *Synth. Met.* **2003**, *137*, 1469.
[24] T. Offermans, S. C. J. Meskers, R. A. J. Janssen, *J. Chem. Phys.* **2003**, *119*, 10 924.
[25] I. Montanari, A. F. Nogueira, J. Nelson, J. R. Durrant, C. Winder, M. A. Loi, N. S. Sariciftci, C. Brabec, *Appl. Phys. Lett.* **2002**, *81*, 3001.
[26] J. Nelson, *Phys. Rev. B* **2003**, *67*, 155 209.
[27] T. J. Savenije, J. E. Kroeze, M. M. Wienk, J. M. Kroon, J. M. Warman, *Phys. Rev. B* **2003**, *69*, 155 205.

